International Journal on Engineering, Science and Technology
Volume 4, Issue 1, 2022 ISSN: 2642-4088

Characterization and Hydrodynamic Evaluation of the Relationship between Permeability and Microstructure Parameters Ceramic Membranes for the Separation of Oil-in-water Emulsion

Florence Aisueni
Robert Gordon University, United Kingdom

Edward Gobina
Robert Gordon University, United Kingdom, e.gobina@rgu.ac.uk

Idris Hashim
Robert Gordon University, United Kingdom

Evans Ogoun
Robert Gordon University, United Kingdom

Abstract: Ceramic membranes for wastewater treatment are usually fine filters prepared by sintering of alumina, titania or zirconia powders at ultra-high temperatures and have an asymmetric cross-section using the same material or a combination of the three giving a base support and an active layer forming the membrane. The Carman–Kozeny (C–K) and Hagen–Poiseuille (H–P) transport equations have been used to predict water permeability of ceramic membranes and can be adapted to take account of the effects of microstructural parameters (porosity, and tortuosity) of ceramic membranes on pure water flux. The hydrodynamics of the membranes were evaluated by gas transport to obtain equivalent water permeability which was then used to obtain the porosity and tortuosity respectively. Gas permeability experiments showed good correspondence with the calculated water flux. Characterization of the membranes was carried out using scanning electron microscopy (SEM) imaging to determine the morphological aspects of the sample including shape and size of membranes while the electron diffraction with x-rays analysis (EDAX) was used to obtain information on the elemental composition.

Keywords: Membrane, Porosity, Tortuosity, Microstructure, Flux

Introduction

Oil refineries produced large quantity of oily wastewater which can also be termed as (O/W) emulsion with oil droplet of different sizes (oil in water or o water in oil emulsion). Offshore oil spillage produces huge amount of oily wastewater (Elanchezhiyan, Sivasurian, & Meenakshi, 2016). This O/W emulsion discharged into the environment directly will not only pollute the environment but reduce water resources especially drinking water. A way to address this problem is to separate oil from water and possibly reuse or recycle both components. Several promising methods have been reported so far by researchers for the separation of oil from O/W emulsions before discharge into the environment, which have their advantages and disadvantages (Wang, Wang, & Geng, 2018). Materials that can meet the challenging requirements of real-world applications are still in the process of development. Hence, there is a need for the advancement of a recyclable, cost -effective, environmentally friend, simple and efficient method that can separate big volumes of O/W emulsions into two phases with high flux and oil rejection rates. These several methods researched and reported for the separation of O/W emulsions are adsorption, electrocoagulation, flocculation, bioremediation, centrifugation, membrane etc (Shi et al., 2019).

These traditional methods are insufficient in the treatment of O/W emulsions due to the small size of oil droplets as well as lower concentrations of oil in water, because below 250mg/L separation is usually not possible (Huang et al., 2018). However, membrane technology has been recently most researched as a promising alternative for the separation of O/W emulsion. This may be because of merit features which includes an excellent combination of longer shelf life, better self-cleaning properties, mechanical, chemical, and thermal strength, survival in organic solvent, low cost, compact design, removal of secondary separation and superior separation factor (Suresh & Pugazhenthi, 2016).

Membranes are commonly classified into two main groups known as polymeric and ceramic membranes. This

classification is grouped based on the material for production of the membranes (C. Li et al., 2020). It has been reported by several authors (Hendren, Brant, & Wiesner, 2009) (Phan et al., 2016) that ceramic membranes have more advantages in chemical, mechanical, and thermal stability, longer shelf life, high membrane flux and formidable corrosive resistance. Based on this, ceramic membrane is receiving recent attention in separation processes for water purification and will be used in this research. Because this research deals with the separation of water across the surface a ceramic membrane and the fact that this microfiltration process deals with sieve effect (W. Li, Xing, & Xu, 2006), hydrodynamic and microstructure (porosity and tortuosity) of the ceramic membrane and how it affects flux is evaluated. The Carman-Kozeny and Hagen-Posseuille equations are expressed in this research to determine the relationship between flux and porosity as well as tortuosity. This research aims at predicting the actual flux of pure water on a ceramic membrane using gas transport while relating this predicted flux to porosity and tortuosity with Carman-Kozeny and Hagen-Poiseuille equations.

Experimental

Morphology and Structure

The microstructure of the unmodified ceramic membrane was analyzed using Scanning Electron Microscope (SEM). Unmodified ceramic membrane samples were placed firmly on a stub and transferred to the sample carousel of the SEM for analysis. The SEM generated images of both outer and inner areas of the sample at 500X, 1000X and 3000X magnifications. The elemental structure of the ceramic membrane was analyzed using Energy dispersive Xray (EDAX).

Crossflow Microfiltration of Pure Water Flux

Pure water from the feed tank was pump into the membrane module as seen in Figure 1, via an inlet tubing using a peristaltic pump at 50L/h at pressure 0.26bar. The water passes through the inlet tubing into the membrane module containing uncoated 6000nm commercial ceramic membrane. Pure water is separated through the ceramic membrane to the permeate received in a graduated beaker place on a weighing balance. This permeate was measured at 10 minutes intervals. The unseparated water passes through the outlet tubing known as the retentate back into the feed. The pure water flux was calculated using the data from filtration with equation 1.

$$J = \frac{V}{A\Delta T} \qquad \text{Equation 1.}$$

Where J denotes the flux of pure water, A(m^2) represents the filtration area of the ceramic membrane, V denotes the permeate volume(L) collected and T(min) represents the filtration time. This calculated flux was confirmed by an extrapolation on gas transport chart where flux was plotted against 1/mean pressure.

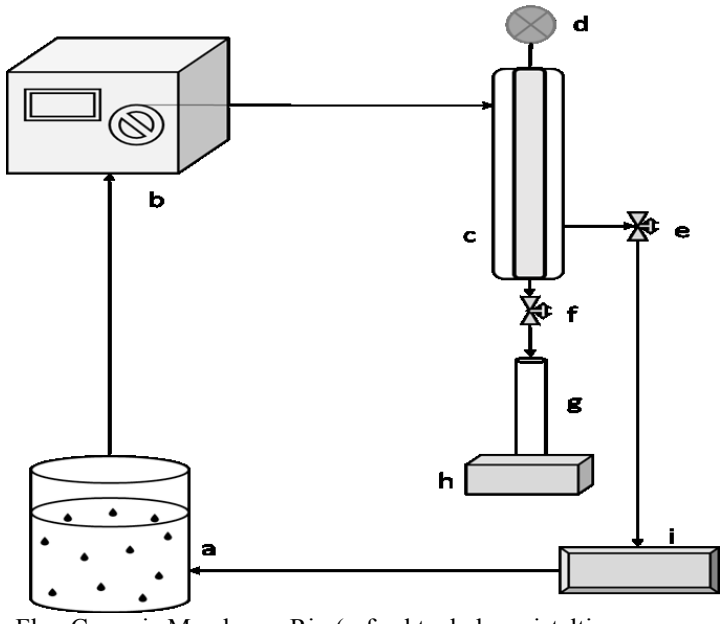

Figure 1. Pure Water Flux Ceramic Membrane Rig (a-feed tank, b-peristaltic pump, c-membrane module, d-pressure gauge, e &f – retentate and permeate valves, g-measuring cylinder, h- weighing balance, i-flowmeter)

Crossflow Gas Transport

Gases (Nitrogen, Argon, and carbon dioxide) were released from the gas cylinder by the regulator through gas tubing into the membrane modules at different pressure drops as seen in Figure 2. The gases permeate through the membrane at different pressures where flowrates were measured out flowrates where measure at standard liter per minute on the flowmeter. The permeated gas escaped into the fume cupboard.

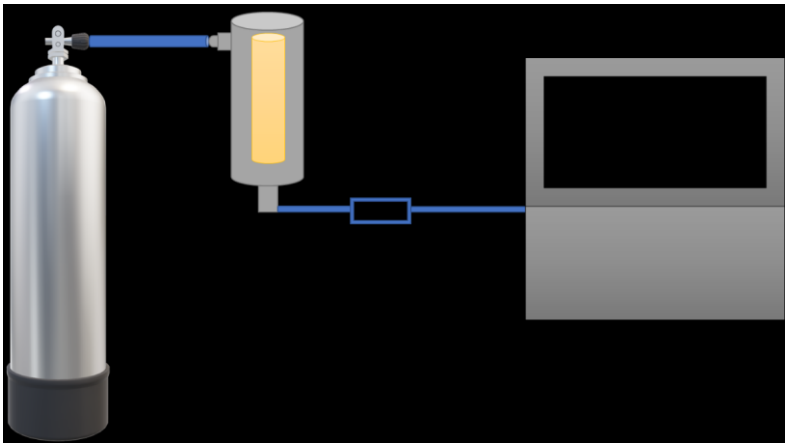

Figure 2: Crossflow Gas Transport (1-Gas cylinder, 2-regulator, 3-tubing, 4-membrane module, 5-flowmeter, 6-fume cupboard)

Microstructure and Flux

The Carmen –Kozeny and Hagen-Poiseuille equations were used to relate the porosity and tortuosity to flux of the ceramic membrane. Flux from the pure water transport calculated from the experiment and porosity calculated using the Archimedes principle from experimental data was imputed in the Hagen-Poiseuille equation to determine tortuosity. Literature equation adapted from Tanko (2018) was also used to predict tortuosity as seen in Figure 3 below.

$$j = \frac{\Delta P d_m^{k2} \varepsilon^3}{k_1 \mu (1-\varepsilon)^2 L}$$ Equation 2

Carmen-Kozeny Equation

$$j = \frac{\Delta P d_m^{k2} \varepsilon}{32 \mu L \tau}$$ Equation 3

Hagen-Poiseuille Equation

$$\frac{\varepsilon}{\tau} = \frac{j \times 32 \mu L}{\Delta P d_m^2}$$ Equation 4

where ΔP, dm is mean pore size, k2 expresses the effect of shape and aggregate style of the specific resistance, Ɛ is the porosity of the layer, k1 is the constant, μ is the viscosity of the feed, and L is the thickness of the ceramic membrane, τ is tortuosity.

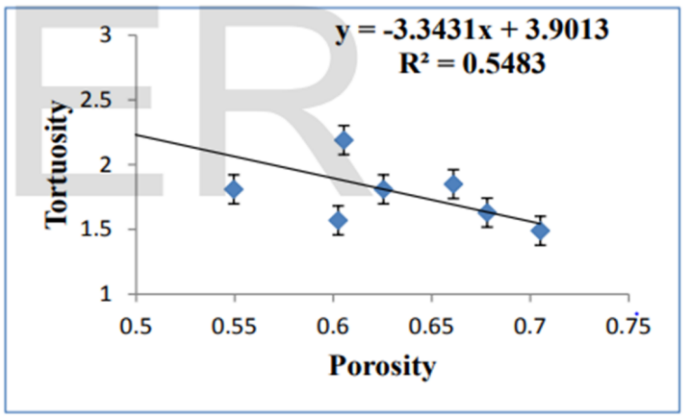

Figure 3. Literaure Equation used to Calculate and Predict Tortuosity (Adapted from Tanko, 2018)

Result and Discussion

Morphology and Structure

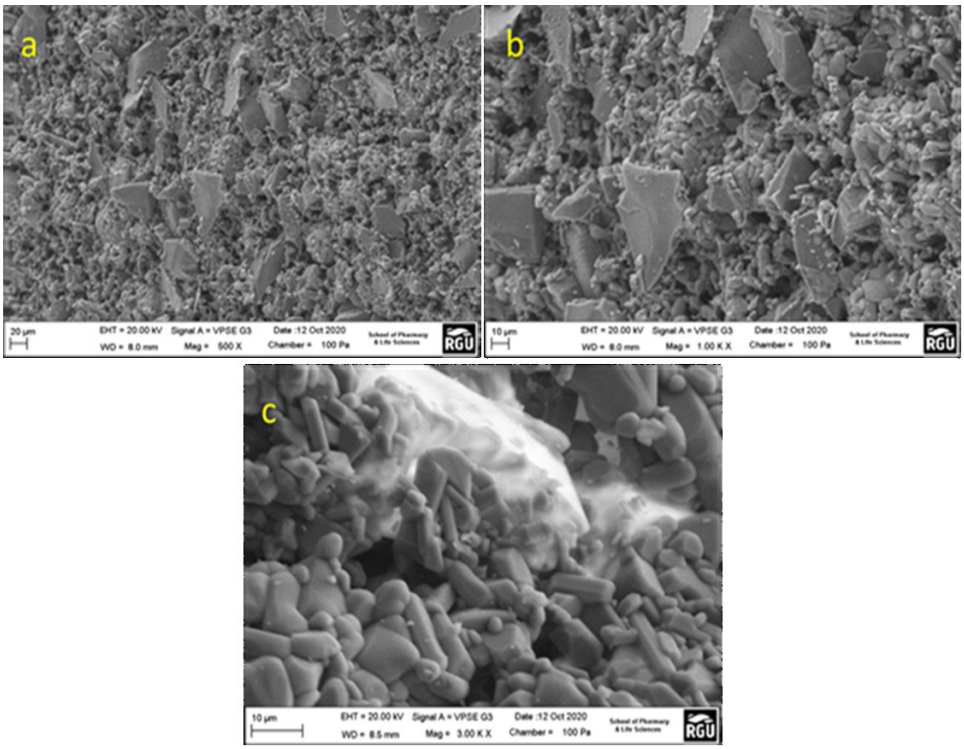

Figure 4. Scanning Electron Microscope (SEM) of Ceramic Membrane

The result from the SEM in Figure 4 shows rough, densely packed uneven particle size and porous membrane. This indicates a range in pore sizes of the membrane that can enhance flux. According to (Gupta et al. 2017) surface roughness in membranes can increase contact angles (Cas) which may increase flux. Evaluation of Support Membrane for Elemental composition using Energy Dispersive X-Ray Analysis (EDAX) in Figure 5 indicates the presence of Zirconia, Iron, Bromine and Titania which are all inorganic elements used for the production of ceramic membrane.

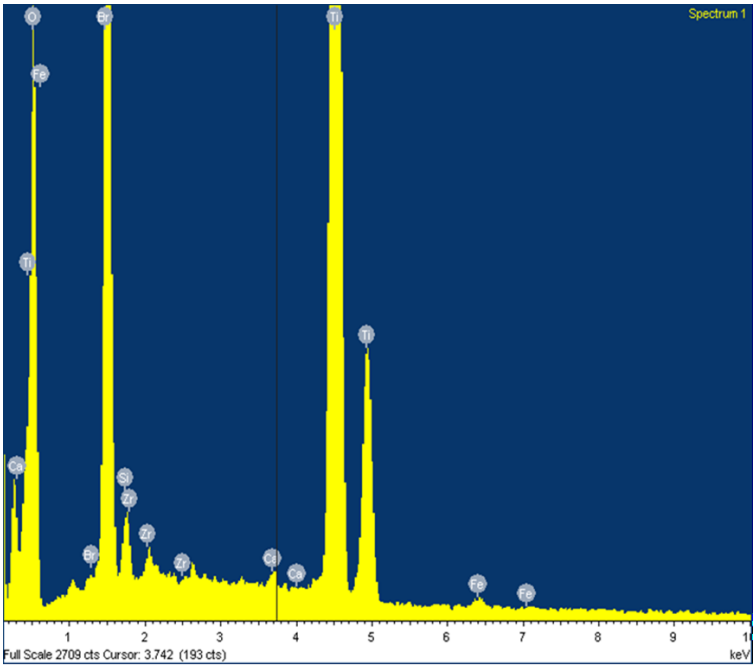

Figure 5. Energy Dispersive Xray of Spectrum of Ceramic Membrane

Crossflow Microfiltration of Pure Water

Equation 1 was used to calculate the flux in Table 1, which gave an approximate of 0.0578(L/m^2.H).

Table 1. Crossflow Pure Water Separation

Pressure (bar)	Time (hr)	Area (m2)	Out (Vol/H)	Flux (L/m2.H)
0.26	0.17	295.96316	16.74	0.056561093
0.26	0.17	295.96316	17.52	0.059196557
0.26	0.17	295.96316	15.66	0.052911991
0.26	0.17	295.96316	17.4	0.058791101
0.26	0.17	295.96316	18.24	0.061629292
0.26	**0.17**	**295.96316**	**17.112**	**0.057818007**

Crossflow Gas Transport

Fluxes of three gases calculated from experimental data using equation1 is represented in table 2 below. The data from the mean is later plotted against 1/mean pressure (1/Pm) and an average intercept from the chart is used to predict the absolute pure water flux seen in Figure 6. This extrapolated absolute pure water flux corresponds with the calculated pure water flux in Table 2.

Table 2. Pure Water Flux

Pressure (bar)	Time (hr)	Area (m2)	Out (Vol/H)	Flux (L/m2.H)
0.26	0.17	295.96316	16.74	0.056561093
0.26	0.17	295.96316	17.52	0.059196557
0.26	0.17	295.96316	15.66	0.052911991
0.26	0.17	295.96316	17.4	0.058791101
0.26	0.17	295.96316	18.24	0.061629292
0.26	**0.17**	**295.96316**	**17.112**	**0.057818007**

Flux was measured by nitrogen, argon and carbon dioxide pure gases and water on the same samples in pressure drop experimental tests, and the followings important results were observed in our study: Flux to carbon dioxide, argon and nitrogen gas was over 10 times larger than that to water using the same membrane specimen. (2) Permeance to all the gases gas were observed to decreases with an increase of differential pore pressure and the relationship between permeability to each gas and the reciprocal of the mean pore pressure was observed to display the Klinkenberg equation (Moghadam & Chalaturnyk, 2014) for most experimental data. Moreover, absolute pure water permeability estimate. (3) Flux to gas shows positive relationship to the differential pore pressure, which can be partially explained by the Darcy Law (Darcy, 1856). Our experimental results therefore suggest that the difference between permeability to gas and water can be explained by the Klinkenberg effect (Moghadam & Chalaturnyk, 2014).

The implication being that if the permeability obtained from experimental measurements using a compressible gas such as nitrogen is substituted for the permeability of water, it is preferable to update the gas permeability using Klinkenberg equation (Moghadam & Chalaturnyk, 2014). Moreover it is better to also include pore pressure or transmembrane pressure drop dependence on both water and gas permeabilities for problems involving fluid flow. If the Klinkenberg effect is to be avoided during steady state gas permeability measurements, then large differential pore pressure above 1 MPa should be used, though this value is not large enough

This is an indication that gas transport can be used as a convenient method for the determination of pure water flux for the separation of O/W emulsion.

Table 3. Gas Transport Flux plotted against 1/Pm

	Flux (L/m^2.H)		
1/Pm	**H^2**	**Ar**	**CO^2**
0.9090909	0.23719168	0.18448242	0.23921896
0.7692308	0.56561093	0.44802873	0.45005601
0.6666667	0.76833887	0.63859299	0.63656571
0.5882353	0.98323048	0.81902085	0.81902085
0.5263158	1.19812209	0.9913396	0.99742143
0.4761905	1.40693186	1.17987657	1.17176746
0.4347826	1.61574163	1.35827716	1.3542226
0.4	1.83063324	1.53667774	1.52451406

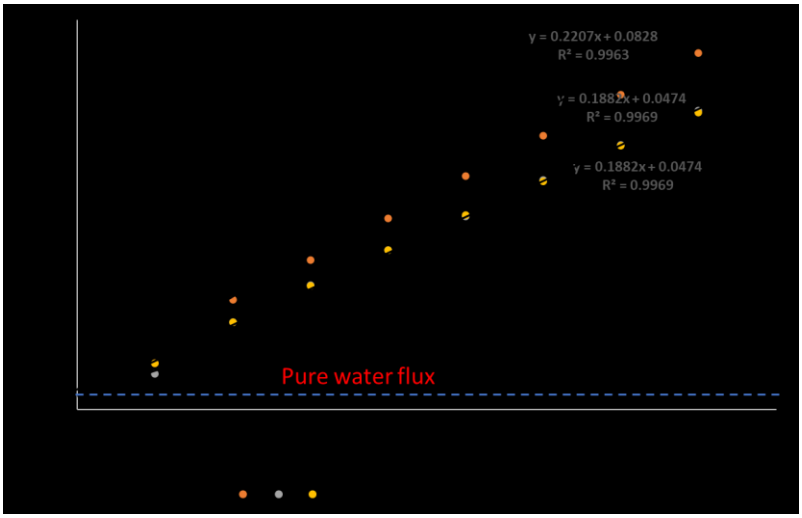

Figure 6. Gas Transport Plotted against 1/Pm to Extrapolate Absolute Pure Water Flux

Microstructure and Flux

From equation 4 calculated using structural experimental data and equation adapted from Tanko (2018), The tortuosity value τ is seen from the Figure 7 respectively. The porosity was measured using Archimedes principle to be 0.04 and using literature data relating porosity and tortuosity a value of 3.77 was obtained for the tortuosity. Furthermore, the Hagen-Poiseuille equation was also used to obtain another estimate for tortuosity which was close to 1. This discrepancy is due to the pore size distribution in the membrane which ranges from 12000nm to 50nm.

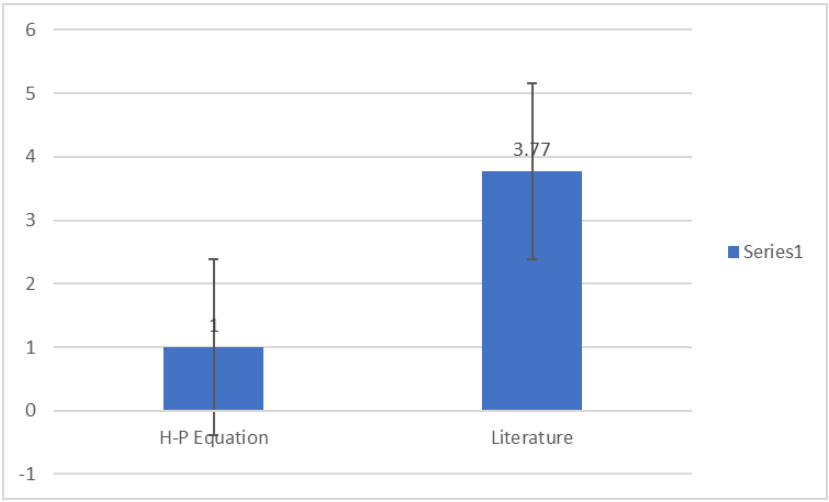

Figure 7. Tortuosity Range between H-P Equation and Literature (Tanko 2018)

Conclusion and Recommendations for Further Work

From the experiments carried out, it can be confirmed that the absolute pure water flux measured corresponds with the value obtained from gas transport measurement. Tortuosity measurement from the Hagen-Poiseuille equation and literature fall with the range of 1-3.77 and this is in range due to the pore size of the ceramic membrane which is a mean pore size, and the actual pore size distribution can be between the range of 50nm-12000nm. The larger the porosity, the smaller the tortuosity and the higher the flux of ceramic membrane.
The next step involved in this research is to undertake some microstructural characterization on the pore size, Thickness and contact angle of the ceramic membrane. Furthermore, undertake some microstructural characterization on the coating of ceramic membrane with aluminum and zinc oxides nanoparticles for surface modification using dip-coating method.

Acknowledgements

We would like thank Robert Gordon University Centre for Process Integration & Membrane Technology, School of Engineering laboratory facilities and study environment provided for this research. We would also like to specialty appreciate Tertiary Education Trust Fund (TETFund) and Petroleum Technology Development Fund (PTDF) and Niger Delta Development Commission (NDDC) all in Nigeria for the Sponsorship required to carry out this research.

References

Darcy, H. (1856). *Les fontaines publiques de la ville de dijon: Exposition et application...* Victor Dalmont.

Elanchezhiyan, S. S., Sivasurian, N., & Meenakshi, S. (2016). Efficacy of La3+ entrapped chitosan bio- polymeric matrix for the recovery of oil from oil- in- water emulsion. *Journal of Applied Polymer Science, 133*(12), n/a. doi:10.1002/app.43218

Hendren, Z., Brant, J., & Wiesner, M. (2009). Surface modification of nanostructured ceramic membranes for direct contact membrane distillation. *Journal of Membrane Science, 331*(1-2), 1-10.

Huang, C., Ko, C., Chen, L., Huang, C., Tung, K., & Liao, Y. (2018). A simple coating method to prepare superhydrophobic layers on ceramic alumina for vacuum membrane distillation. *Separation and Purification Technology, 198*, 79-86.

Li, C., Feng, G., Pan, Z., Song, C., Fan, X., Tao, P., . . . Zhao, S. (2020). High-performance electrocatalytic microfiltration CuO/Carbon membrane by facile dynamic electrodeposition for small-sized organic pollutants removal. *Journal of Membrane Science, 601*, 117913.

Li, W., Xing, W., & Xu, N. (2006). Modeling of relationship between water permeability and microstructure parameters of ceramic membranes. *Desalination, 192*(1-3), 340-345.

Moghadam, A. A., & Chalaturnyk, R. (2014). Expansion of the klinkenberg's slippage equation to low permeability porous media. *International Journal of Coal Geology, 123*, 2-9.

Phan, H. V., McDonald, J. A., Hai, F. I., Price, W. E., Khan, S. J., Fujioka, T., & Nghiem, L. D. (2016). Biological performance and trace organic contaminant removal by a side-stream ceramic nanofiltration membrane bioreactor. *International Biodeterioration & Biodegradation, 113*, 49-56.

Shi, L., Lei, Y., Huang, J., Shi, Y., Yi, K., & Zhou, H. (2019). Ultrafiltration of oil-in-water emulsions using ceramic membrane: Roles played by stabilized surfactants. *Colloids and Surfaces A: Physicochemical and Engineering Aspects, 583*, 123948.

Suresh, K., & Pugazhenthi, G. (2016). Development of ceramic membranes from low-cost clays for the separation of oilâ€“water emulsion. *Desalination and Water Treatment, 57*(5), 1927-1939.

Tanko, N. L. (2018). The effect of Porosity on Tortuosity. *International Journal of Scientific & Engineering Research, 9(5),* 2163-2169

Wang, J., Wang, H., & Geng, G. (2018). Highly efficient oil-in-water emulsion and oil layer/water mixture separation based on durably superhydrophobic sponge prepared via a facile route. *Marine Pollution Bulletin, 127*, 108-116.